LONGITUDINAL PHASE SPACE TOMOGRAPHY WITH SPACE CHARGE

S. Hancock, M. Lindroos, CERN, Geneva, Switzerland
S. Koscielniak, TRIUMF, Vancouver, Canada

Abstract

The tomographic reconstruction of longitudinal phase space density is a hybrid measurement technique which incorporates particle tracking. Hitherto, a very simple tracking algorithm has been employed because only a brief span of measured bunch profile data is required to build a snapshot of phase space. This is one of the strengths of the method, as tracking for relatively few turns relaxes the precision to which input machine parameters need to be known. The recent addition of longitudinal space charge considerations as an optional refinement of the code is now described. Simplicity suggested an approach based on the derivative of bunch shape with the properties of the vacuum chamber parametrized by a single value of distributed reactive impedance and by a geometrical coupling coefficient. This is sufficient to model the dominant collective effects in machines of low to moderate energy. In contrast to simulation codes, binning is not an issue since the profiles to be differentiated are measured ones. Results obtained with and without the inclusion of space charge are presented and compared for a proton beam case in the CERN PS Booster (PSB).

1 INTRODUCTION

Longitudinal phase space tomography[1,2,3] takes into account the non-linearities of synchrotron motion by tracking test particles in order to build maps which describe the evolution of phase space. The maps are used to reconstruct iteratively a distribution whose projections converge towards the measured bunch profiles. The tracking can be made arbitrarily complex. In particular, collective effects due to the interaction of the beam with a wideband reactive impedance are readily included since the wakefield may be modelled in terms of the derivative of bunch shape and this is known from the measured data. The test particles that are tracked are *not* binned to obtain bunch profiles.

2 TRACKING

Particles are tracked turn by turn by iterating standard difference equations[4]. To a good approximation, the relative rf phase of the ith particle as it crosses the cavity gap to complete the mth turn is

$$\Delta\phi_{i,m+1} = \Delta\phi_{i,m} - 2\pi h\left(\frac{\eta_{0,m}\Delta E_{i,m}}{\beta_{0,m}^2 E_{0,m}}\right) \qquad (1)$$

where ΔE_i is its energy with respect to that, E_0, of the synchronous particle, h is the harmonic number of the rf, and where η_0, β_0 are, respectively, the phase slip factor and relativistic speed of the synchronous particle.

Assuming negligible modification of the synchronous phase due to self-fields, the corresponding energy increment at the end of the mth turn yields

$$\Delta E_{i,m+1} = \Delta E_{i,m} + q[V_{rf,m+1}(\phi_{0,m+1} + \Delta\phi_{i,m+1}) - V_{rf,m+1}(\phi_{0,m+1}) + V_{self,m+1}(\phi_{0,m+1} + \Delta\phi_{i,m+1})] \qquad (2)$$

where q is the charge carried by the particle, ϕ_0 is the synchronous phase, and where V_{rf}, V_{self} are the applied rf and self-field voltage functions, respectively. The latter may be written[5] in terms of the line charge density, $q\lambda$, along the bunch

$$V_{self,m}(\phi) = qh^2\omega_{0,m}\left[\frac{gZ_{vacuum}}{2\beta_{0,m}\gamma_{0,m}^2} - \left|\frac{Z_{wall}}{n}\right|\right]\frac{d\lambda_m(\phi)}{d\phi}$$

where $h\omega_0$ is the rf frequency and γ_0 is the relativistic energy of the synchronous particle. The factor in square brackets is the effective impedance seen by the beam and comprises a direct space charge term (which is expressed in terms of a geometrical coupling coefficient, g, and the impedance of free space, Z_{vacuum}) and the distributed impedance of the vacuum chamber, $|Z_{wall}|$ (divided by the mode number, n).

Equations (1) and (2) together constitute the turn-by-turn tracking used in the code. However, since the line charge density is not necessarily known at every turn, the self-field voltage is evaluated from the mean of the nearest two bunch profile measurements. Smoothing and differentiation are achieved using a Savitzky-Golay filter[6] of order 4.

3 DISCUSSION

The action of a phase loop is not included in the tracking. Typically, closed-loop conditions do not affect the bunch during a measurement span, unless its dipole motion or the filamentation of a badly matched distribution would otherwise have shifted the barycentre of the observed profiles.

Equation (1) takes the ratio of synchronous revolution periods on consecutive turns to be unity, which is a good approximation except at very low energies. Furthermore, the orbit expansion is only made to first order in fractional energy offset, so that reconstructing near transition should be avoided. This is anyway true since the lack of phase space motion near transition precludes tomography.

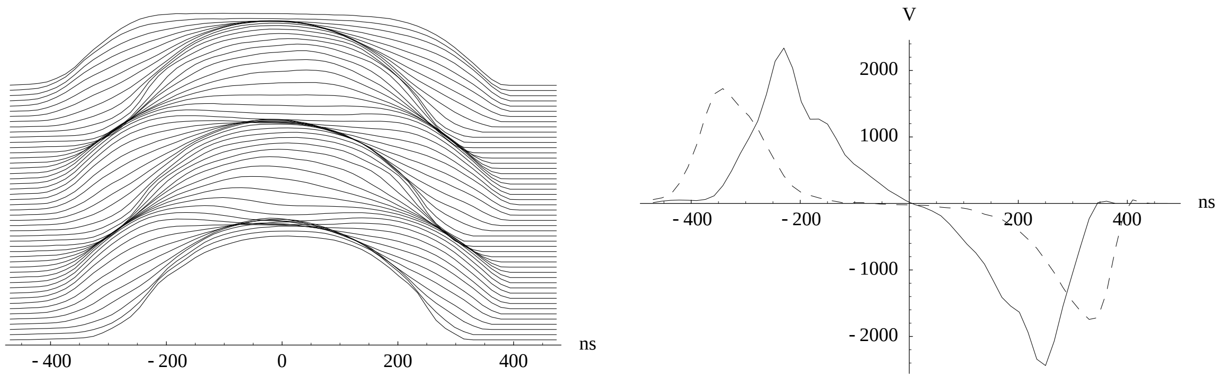

(i) (ii)

Figure 1: (i) Bunch shape oscillations of 6.5×10^{12} protons measured every 16 turns after an abrupt reduction in the second-harmonic component of a stationary dual-harmonic bucket at 100 MeV in the PSB. (ii) Corresponding self-field voltage functions obtained from the mean derivative of the first two (solid line) and last two (dashed line) profiles.

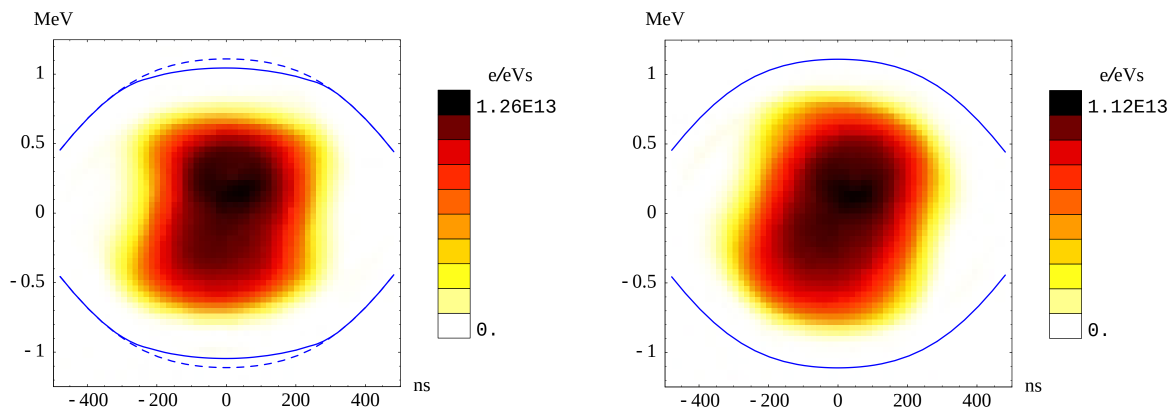

(i) (ii)

Figure 2: Phase space reconstructions (i) with and (ii) without space charge. Note the different density scales.

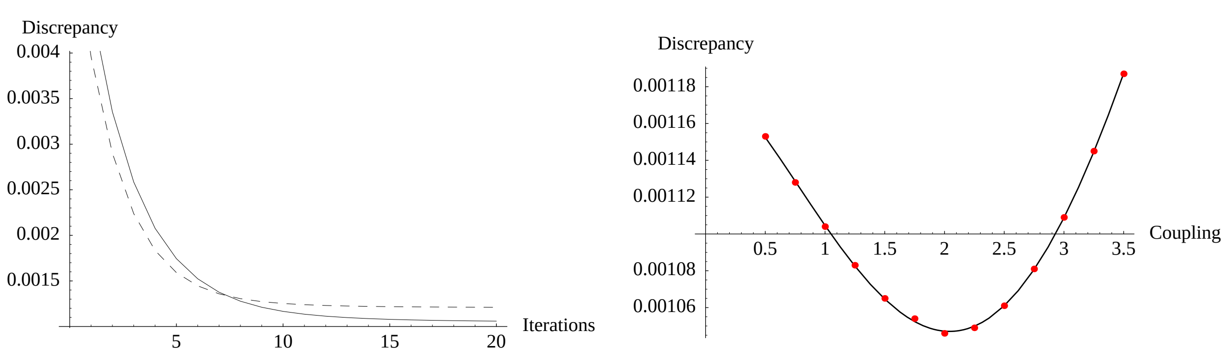

(i) (ii)

Figure 3: (i) Convergence for the two cases of Fig. 2; the solid line is with space charge included.
(ii) Discrepancy (after 50 iterations) versus geometrical coupling.

Since it is not dissipative, a pure reactive impedance cannot alter the average energy of the bunch nor, in the absence of coherent motion, is there any modification of the synchronous phase. Equation (2) takes the self-field voltage to be zero at ϕ_0. This simplification guarantees the convergence of the root-finding algorithm that is used to evaluate ϕ_0 and it assumes that the average energy of the bunch is in equilibrium at E_0. Typically, this implies only a small error with respect to the true centre of individual particle motion and the method is known to be very tolerant of such errors. No resistive (in-phase) component of the self-field voltage is considered.

For a circular beam of radius a in a circular pipe of radius b, the coupling coefficient of the particle ensemble may be estimated[7] as $g = 0.5 + 2\ln(b/a)$. In the absence of cylindrical symmetry, the situation is more complicated, but the direct space charge component can still be expressed in terms of this single input parameter.

4 DISCREPANCY

Discrepancy[8] expresses in a single figure of merit the residual bin-by-bin differences between the projections of a reconstructed distribution and the original profiles,

$$d = \sqrt{\frac{1}{M} \sum_{\forall i \ni N_i > 0} (e_i - r_i)^2 / N_i}$$

Here, e_i and r_i are, respectively, the measured and reconstructed contents of the ith bin and M is the number of terms in the summation. The weighting factor N_i is the number of image pixels that project into the ith bin. However, since each e_i constitutes an independent measurement whose variance is dominated by noise and is therefore the same for all i, the expression can be modified slightly so that d^2 becomes more like the mean χ^2 per bin. Thus,

$$d' = \sqrt{\frac{1}{M'} \sum_{i=1}^{M'} (e_i - r_i)^2}$$

where M' is the total number of bins in all profiles. It is this form of discrepancy that is implemented in the code for monitoring convergence.

5 SOME RESULTS

The mountain range data of Fig. 1(i) are tomographically reconstructed in Fig. 2 with and without the inclusion of space charge. The images correspond to the time of the first measured profile, i.e., to a minimum of bunch length, but the reconstructed distribution is only fully upright when space charge is taken into account. The dashed bucket separatrix illustrates the loss of acceptance. The coupling coefficient was estimated as g=1.8 from beamscope[9] measurements of transverse beam size, whereas g=2.0 produced the best reconstructed image (see Fig. 3). Since the beamscope is known to overestimate the horizontal size of the beam, the larger value of g was adopted. This corresponds to a space charge impedance of more than 700 Ω. Since the inductive wall impendance of the PSB is considerably less than this, it was simply taken to be zero.

The deliberately mismatched bunch generates a varying self-field voltage (see Fig. 1(ii)) which can therefore be distinguished from a mere calibration error of the rf voltages. When space charge was included, discrepancy minima were obtained in good agreement with the measured cavity voltages on both harmonics.

6 CONCLUSIONS

A proven technique for longitudinal phase space tomography has been refined to include collective effects due to direct space charge and reactive wall impedance.

A poorly known parameter in the physical model of the hybrid algorithm may be estimated by maximizing the resultant image quality as a function of that parameter. The space charge impedance of the PSB has effectively been measured in this way under conditions contrived to induce a strong space charge effect.

ACKNOWLEDGEMENTS

The authors wish to thank Fred James for helpful discussions on the statistics of correlated and uncorrelated data and Mike Metcalf for advice on programming in Fortran 95.

REFERENCES

[1] http://home.cern.ch/t/tomograp/www/

[2] S. Hancock, P. Knaus, M. Lindroos, “Tomographic measurements of longitudinal phase space density”, in Proc. European Particle Accelerator Conf., Stockholm, 1998.

[3] S. Hancock, M. Lindroos, E. McIntosh, M. Metcalf, “Tomographic measurements of longitudinal phase space density”, Computer Physics Communications, 118, pp61-70 (1999).

[4] J. MacLachlan, “Difference equations for longitudinal motion in a synchrotron”, FNAL, FN-529 (1989).

[5] S. Hansen, H.G. Hereward, A. Hofmann, K. Hubner, S. Myers, “Effects of space charge and reactive wall impedance on bunched beams”, IEEE Trans. Nucl. Sci., NS-22, pp1381-1384 (1975).

[6] A. Savitzky, M.J.E. Golay, “Analytical Chemistry”, vol. 36, pp1627-1639 (1964).

[7] R. Baartman, “Form factor g in longitudinal space charge impedance”, TRIUMF Kaon Factory Project Definition Study, TRI-DN-92-K206 (1992).

[8] R. Gordon, “A tutorial on ART”, IEEE Trans. Nucl. Sci., NS-21, pp78-93, 1974.

[9] H. Schonauer, “Experience with the beamscope emittance measurement system at the CERN PS Booster”, CERN/PS 92-10(HI) (1992).